Sigma versus Pi Interactions in Alkali Metal Ion Binding to Azoles: Threshold Collision-Induced Dissociation and ab Initio Theory Studies

H. Huang and M. T. Rodgers*

Department of Chemistry, Wayne State University, Detroit, Michigan 48202

Received: September 26, 2001; In Final Form: February 13, 2002

Threshold collision-induced dissociation of M^+(azole) with xenon is studied by guided ion beam mass spectrometry. M^+ include the following alkali metal ions: Li^+, Na^+, and K^+. The azoles studied include pyrrole, 1-methylpyrrole, pyrazole, 1-methylpyrazole, and 1-methylimidazole. In all cases, endothermic loss of the intact neutral azole is observed as the primary reaction pathway. Minor production of M^+Xe formed by ligand exchange is also observed. The cross-section thresholds are interpreted to yield 0 and 298 K binding energies for M^+−azole after accounting for the effects of multiple ion-neutral collisions, internal energy of the reactant ions, and dissociation lifetimes. Ab initio calculations at MP2(full)/6-31G* level of theory are used to determine the structures of these complexes and provide molecular constants necessary for the thermodynamic analysis of the experimental data. Single-point calculations at the MP2(full)/6-311+G(2d,2p) level using the MP2(full)/6-31G* optimized geometries are used to obtain theoretical bond dissociation energies. Zero-point energy and basis set superposition error corrections are also included. Excellent agreement between theory and experiment is found for the Na^+ and K^+ systems, whereas the theoretical bond dissociation energies to the Li^+ systems are systematically low. The calculated and measured bond dissociation energies are compared among the systems examined here and to previous values from the literature, to determine the influence that the metal ion, the nature of the binding interaction (π vs σ binding), and the dipole moment, quadrupole moment, and polarizability of the ligand have on the strength of the binding in these complexes.

Introduction

Much of our recent work has focused on the development and application of quantitative threshold collision-induced dissociation (CID) methods to obtain accurate thermodynamic information on a variety of organic, organometallic, and biologically relevant metal−ligand complexes.[1−15] Our interest in extending these techniques to a much broader class of ligands and also much larger ligands has provided the driving force for this work. Such reliable thermodynamic information can be employed in a variety of ways. First and foremost, such measurements allow the intrinsic interactions between the metal ion and the ligand to be examined in detail. Second, such absolute thermochemical information can be employed as reference anchors for experimental studies where only relative thermodynamic information can be obtained, e.g., for many equilibrium and kinetic method studies. In addition, this thermochemistry can be employed as benchmarks to enhance or extend the accuracy of computational techniques to a larger variety of systems.

In the present study, we examine the interactions of alkali metal ions with a variety of azoles. The azoles are members of the class of five-membered heteroaromatic compounds referred to as π-excessive N-heterocycles.[16] The particular systems examined here are chosen as models of noncovalent interactions with nucleic acids and possibly of selective cation transport through biological membranes.[17,18] The azoles are also the building blocks for many antibiotics, anticancer agents, fungicides, and drugs.[19−23] The azoles also play important roles as high energy density compounds useful in explosives and fuels[24,25] and as clean sources of nitrogen in thin film deposition.[26−29]

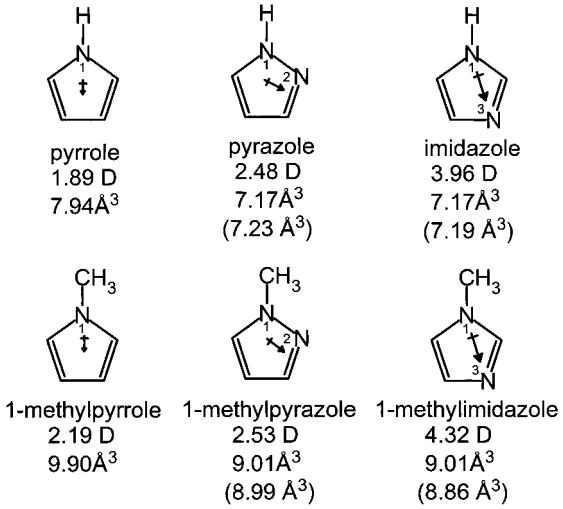

Figure 1. Structures of the azole molecules. Properly scaled dipole moments in Debeye are shown as arrows. Values listed are determined from theoretical calculations performed here. Molecular polarizabilities in Å^3, taken from Miller, are also shown.[30] Values listed are estimations from an additivity method, and experimental values are given in parentheses.

In the present study, guided ion beam mass spectrometry is used to collisionally excite complexes of Li^+, Na^+, and K^+ bound to five different azoles: pyrrole, 1-methylpyrrole, pyrazole, 1-methylpyrazole, and 1-methylimidazole. The structures of the azoles, including imidazole examined in a previous study,[6] are shown in Figure 1 along with their calculated dipole

* To whom correspondence should be addressed.

10.1021/jp013630b CCC: $22.00
Published on Web 04/02/2002

moments (determined here) and measured and estimated polarizabilities.[30] The kinetic energy-dependent cross sections for the CID processes are analyzed by methods developed previously.[4] The analysis explicitly includes the effects of the internal and translational energy distributions of the reactants, multiple ion-neutral collisions, and the lifetime for dissociation. We derive M^+−azole bond dissociation energies (BDEs) for all of the complexes and compare these results to previous literature values available for several of these azoles to H^+ and Li^+ obtained in FT-ICR equilibrium studies[31−33] and to the ab initio calculations performed here and in the literature.[6,8,34−36]

Because the nitrogen present in the ring has a larger electronegativity than carbon, this leads to a disturbance in the symmetry of the π-electron system, localizing more negative charge on nitrogen atom(s) both above and in the plane of the molecule than above the carbon atoms. This leads to two competitive electrostatic binding modes in such molecules, σ binding to the lone pair of electrons on a nitrogen atom (dipole moment) and π binding to the π-electron density of the aromatic ring (quadrupole moment). Pyrrole and 1-methylpyrrole possess only a single nitrogen atom that does not have a lone pair of electrons in the plane of the molecule; thus there is only one favorable binding mode. The alkali metal cation interacts with the quadrupole moment produced by the π-electron cloud of the five-membered ring and sits above the plane of the ring. In contrast, pyrazole, 1-methylpyrazole, imidazole, and 1-methylimidazole each have two nitrogen atoms, one of which possesses a lone pair of electrons in the plane of the molecule, and therefore both types of binding may occur. The M^+(azole) complexes studied here are chosen to elucidate the influence that the metal ion, the nature of the binding interaction (π vs σ binding), and the dipole moment, quadrupole moment, and polarizability of the ligand have on the strength of the binding in these complexes. In addition, the π binding M^+(azole) complexes are compared to the analogous M^+(benzene)[37] and M^+(toluene)[38] systems to examine the influence of the nitrogen atom(s) on the strength of the cation−π interaction.

Experimental Section

General Procedures. Cross sections for collision-induced dissociation of M^+(azole), where $M^+ = Li^+$, Na^+, and K^+ and azole = pyrrole, 1-methylpyrrole, pyrazole, 1-methylpyrazole, and 1-methylimidazole, are measured using a guided ion beam tandem mass spectrometer that has been described in detail previously.[1] The M^+(azole) complexes are generated as described below. The ions are extracted from the source, accelerated, and focused into a magnetic sector momentum analyzer for mass analysis. Mass-selected ions are decelerated to a desired kinetic energy and focused into an octopole ion guide, which traps the ions in the radial direction.[39] The octopole passes through a static gas cell containing xenon, used as the collision gas, for reasons described elsewhere.[40−42] Low gas pressures in the cell (typically 0.05−0.20 mTorr) are used to ensure that multiple ion-neutral collisions are improbable. Product and unreacted beam ions drift the end of the octopole where they are focused into a quadrupole mass filter for mass analysis and subsequently detected with a secondary electron scintillation detector and standard pulse-counting techniques. The detection of Li^+ products presents more difficulty than higher mass ions because the Li^+ peak overlaps with the zero-blast signal. The zero-blast intensity is typically large compared to the Li^+ intensity. Although in principle background subtraction should eliminate intensity arising from the zero blast in the Li^+ signal, in practice mismatch in intensity can occur and introduce error in the threshold determination. This difficulty can be improved or eliminated by increasing the radio frequency of the quadrupole, which can only be accomplished by replacing the resonator electronics of the quadrupole mass filter.

Ions intensities are converted to absolute cross sections as described previously.[43] Absolute uncertainties in cross-section magnitudes are estimated to be ±20%, which are largely the result of errors in the pressure measurement and the length of the interaction region. Relative uncertainties are approximately ±5%. Because the radio frequency used for the octopole does not trap light masses with high efficiency, the cross sections for Li^+ products are more scattered and show more variations in magnitude than is typical for heavier ions. Therefore, absolute magnitudes of the cross sections for production of Li^+ are probably accurate to ±50%. This difficulty in trapping of Li^+ should not influence our ability to determine the thresholds for these products because at or near threshold the Li^+ ions will have little or no radial velocity and therefore are efficiently transferred to the detector. Ion loss increases with energy and thus the cross sections appear slower rising than for the Na^+ and K^+ products.

Ion kinetic energies in the laboratory frame, E_{lab}, are converted to energies in the center-of-mass frame, E_{CM}, by use of the formula $E_{CM} = E_{lab}m/(m + M)$, where M and m are the masses of the ionic and neutral reactants, respectively. All energies reported below are in the CM frame unless otherwise noted. The absolute zero and distribution of the ion kinetic energies are determined using the octopole ion guide as retarding potential analyzer, as previously described.[43] The distribution of the ion kinetic energies is nearly Gaussian with a full width at half-maximum (fwhm) typically between 0.2 and 0.5 eV (lab) for these experiments. The uncertainty in the absolute energy scale is ±0.05 eV (lab).

Even when the pressure of the reactant neutral is low, it has previously been demonstrated that the effects of multiple collisions can significantly influence the shape of CID cross sections.[44] Because the presence and magnitude of these pressure effects is difficult to predict, we have performed pressure-dependent studies of all cross sections examined here. In the present systems, we observe small cross sections at low energies that have an obvious dependence on pressure. We attribute this to multiple energizing collisions that lead to an enhanced probability of dissociation below threshold as a result of the longer residence time of these slower moving ions. Data free from pressure effects are obtained by extrapolating to zero reactant pressure, as described previously.[44] Thus, results reported below are due to single bimolecular encounters.

Ion Source. The M^+(azole) complexes are formed in a 1-m long flow tube[1] operating at a pressure of 0.6−1.1 Torr with a helium flow rate of 2000−7000 sccm. Metal ions are generated in a continuous dc discharge by argon ion sputtering of a cathode, made from tantalum with a cavity carrying the alkali metal. Typical operating conditions of the discharge for alkali metal ion production are 2−3.5 kV and 20−35 mA in a flow of roughly 10% argon in helium. The M^+(azole) complexes are formed by condensation of the alkali metal ion with the neutral azole, which is introduced into the flow 20−50 cm downstream from the dc discharge. Although the vapor pressure of all of the azole ligands was sufficient to carry out these experiments, increased ion signals were obtained by flowing helium through the sample using a midget bubbler. The flow conditions used in this ion source provide in excess of 10^5 collisions between an ion and the buffer gas, which should thermalize the ions both vibrationally and rotationally. In our analysis of the data,

we assume that the ions produced in this source are in their ground electronic states and that the internal energy of the M^+(azole) complexes is well described by a Maxwell−Boltzmann distribution of ro-vibrational states at 300 K. Previous work from this[1,3,8,9,11−14] and the Armentrout laboratories has shown that these assumptions are generally valid.[40,44−48]

Thermochemical Analysis. The threshold regions of the reaction cross sections are modeled using eq 1,

$$\sigma(E) = \sigma_0 \sum_i g_i (E + E_i - E_0)^n / E \qquad (1)$$

where σ_0 is an energy-independent scaling factor, E is the relative kinetic energy of the reactants, E_0 is the threshold for reaction of the ground electronic and ro-vibrational state, and n is an adjustable parameter. The summation is over the ro-vibrational states of the reactant ions, i, where E_i is the excitation energy of each state and g_i is the population of those states ($\Sigma g_i = 1$). The populations of excited ro-vibrational levels are not negligible even at 298 K as a result of the many low-frequency modes present in these ions. The relative reactivity of all ro-vibrational states, as reflected by σ_0 and n, is assumed to be equivalent.

The Beyer−Swinehart algorithm[49] is used to evaluate the density of the ro-vibrational states, and the relative populations g_i are calculated by an appropriate Maxwell−Boltzmann distribution at the 298 K temperature appropriate for the reactants. The vibrational frequencies of the reactant complexes are determined from ab initio theory calculations as discussed below. The average vibrational energies at 298 K of the M^+(azole) complexes are given in the Supporting Information in Table S1. We have estimated the sensitivity of our analysis to the deviations from the true frequencies by scaling the calculated frequencies to encompass the range of average scaling factors needed to bring calculated frequencies into agreement with experimentally determined frequencies found by Pople et al.[50] Thus, the calculated scaled vibrational frequencies were increased and decreased by 10%. The corresponding change in the average vibrational energy is taken to be an estimate of 1 standard deviation of the uncertainty in the vibrational energy (Table S1) and is included in the uncertainties, also reported as one standard deviation, listed with the E_0 values.

We also consider the possibility that collisionally activated complex ions do not dissociate on the time scale of our experiment (about 10^{-4} s) by including statistical theories for unimolecular dissociation, specifically Rice−Ramsperger−Kassel−Marcus (RRKM) theory, into eq 1 as described in detail elsewhere.[4,47] This requires sets of ro-vibrational frequencies appropriate for the energized molecules and the transition states (TS) leading to dissociation. The former sets are given in Tables S1 and S2. We assume that the TSs are loose and productlike because the interaction between the alkali metal ion and the azole ligand is largely electrostatic. In this case, the TS model used corresponds to a phase space limit (PSL) that has been described in detail elsewhere.[4] Briefly, the vibrations used to model the TSs are the frequencies corresponding to the products, which are also found in Table S1. The transitional frequencies, those that become rotations of the completely dissociated products, are treated as rotors. For the M^+(azole) complexes, the two transitional mode rotors have rotational constants equal to those of the neutral azole product with axes perpendicular to the reaction coordinate. These are listed in Table S2. The external rotations of the energized molecule and TS are also included in the modeling of the CID data. The external rotational constants of the TS are determined by assuming that the TS occurs at the centrifugal barrier for interaction of M^+ with the neutral azole, calculated variationally as outlined elsewhere.[4] The 2D external rotations are treated adiabatically but with centrifugal effects included, consistent with the discussion of Waage and Rabinovitch.[51] In the present work, the adiabatic 2D rotational energy is treated using a statistical distribution with explicit summation over the possible values of the rotational quantum number, as described in detail elsewhere.[4]

The model represented by eq 1 is expected to be appropriate for translationally driven reactions[52] and has been found to reproduce reaction cross sections well in a number of previous studies of both atom−diatom and polyatomic reactions,[53,54] including CID processes.[1−15,40,44,46,47,55−57] The model is convoluted with the kinetic energy distributions of both reactants, and a nonlinear least-squares analysis of the data is performed to give optimized values for the parameters σ_0, E_0, and n. The error associated with the measurement of E_0 is estimated from the range of threshold values determined for different zero-pressure extrapolated data sets, variations associated with uncertainties in the scaled vibrational frequencies, and the error in the absolute energy scale, 0.05 eV (lab). For analyses of Li^+ products an additional contribution to the error arises from difficulties associated with the efficient detection of this light mass ion as described above. For analyses that include the RRKM lifetime effect, the uncertainties in the reported E_0 values also include the effects of increasing and decreasing the time assumed available for dissociation (or equivalently, the distance traveled between the collision and detection) by a factor of 2.

Equation 1 explicitly includes the internal energy of the ion, E_i. All energy available is treated statistically, which should be a reasonable assumption because the internal (rotational and vibrational) energy of the reactants is redistributed throughout the ion upon impact with the collision gas. The threshold for dissociation is by definition the minimum energy required leading to dissociation and thus corresponds to formation of products with no internal excitation. The assumption that products formed at threshold have an internal temperature of 0 K has been tested for several systems.[3,5,7,40,41,46,47] It has also been shown that treating all energy of the ion (vibrational, rotational, and translational) as capable of coupling into the dissociation coordinate leads to reasonable thermochemistry. The threshold energies for dissociation reactions determined by analysis with eq 1 are converted to 0 K BDEs by assuming that E_0 represents the energy difference between reactants and products at 0 K.[58] This assumption requires that there are no activation barriers in excess of the endothermicity of dissociation. This is generally true for ion−molecule reactions[53] and should be valid for the simple heterolytic bond fission reactions examined here.[59]

Ab Initio Calculations. To obtain model structures, vibrational frequencies, and energetics for the neutral, protonated, and metalated azole, ab initio calculations were performed using Gaussian 98.[60] Geometry optimizations were performed at the MP2(full)/6-31G* level.[61] Vibrational analyses of the geometry-optimized structures were performed to determine the vibrational frequencies of all geometry-optimized structures. When used to model the data or to calculate thermal energy corrections, the MP2(full)/6-31G* vibrational frequencies are scaled by a factor of 0.9646.[62] The scaled vibrational frequencies thus obtained for all systems calculated (the corresponding imidazole systems and the protonated systems were also calculated here) are available as Supporting Information and listed in Table S1, whereas Table S2 lists the rotational constants. Single-point calculations were carried out at the MP2(full)/6-311+G(2d,2p)

level using the MP2(full)/6-31G* optimized structures. To obtain accurate BDEs, zero-point energy (ZPE) corrections were applied and basis-set superposition errors (BSSE) were subtracted from the computed dissociation energies in the full counterpoise approximation.[63,64] The ZPE corrections vary with the cation such that the corrections are largest for the H^+ complexes (31.7−36.0), are significantly small for the Li^+ complexes (5.1−7.8 kJ/mol), somewhat smaller for the Na^+ complexes (3.4−4.6 kJ/mol), and even smaller for the K^+ complexes (2.6−3.7 kJ/mol). Similarly, the BSSE corrections are small and vary with the cation such that the corrections are of similar magnitude for the H^+, Li^+, and Na^+ complexes (5.9−9.9 kJ/mol) and somewhat smaller for the K^+ complexes (3.7−5.6 kJ/mol).

Results

Cross Sections for Collision-Induced Dissociation. Experimental cross sections were obtained for the interaction of Xe with 15 M^+(azole) complexes, where $M^+ = Li^+$, Na^+, and K^+ and azole = pyrrole, 1-methylpyrrole, pyrazole, 1-methylpyrazole, and 1-methylimidazole. Figure 2 shows representative data for 1-methylimidazole with all three alkali metal ions. A set of figures for the remaining 12 M^+(azole) complexes is available in the Supporting Information as Figure S1. As discussed above, the dependence of the cross sections on pressure observed in the M^+ product data at the lowest energies, Figure 2, are a consequence of multiple collisions. A true single-collision cross section is obtained when the data are extrapolated to zero pressure of the Xe reactant as shown in Figure 2. The other M^+(azole) complexes show similar relative behavior. The most favorable process for all complexes is the loss of the intact azole molecule in the CID reaction:

$$M^+(\text{azole}) + \text{Xe} \rightarrow M^+ + \text{azole} + \text{Xe} \qquad (2)$$

The magnitudes of the cross sections generally increase in size from $M^+ = Li^+$ to Na^+ to K^+. This is largely because the thresholds decrease in the same order. The only other product that is observed in the interaction of these complexes with Xe is the result of a ligand exchange process to form M^+Xe. The cross sections for these products are 1−2 orders of magnitude smaller than those for the primary dissociation product, M^+, and the thresholds are slightly lower (by the M^+−Xe binding energy). As little systematic information can be gleaned from these products, they will not be discussed further. However, it is conceivable that this ligand exchange pathway might cause a competitive shift in the observed thresholds. We do not believe such competition is likely to affect our threshold measurements in any of these systems, within the quoted experimental errors, for several reasons that have been detailed elsewhere.[57]

Threshold Analysis. The model of eq 1 was used to analyze the thresholds for reactions 2 in the 15 M^+(azole) systems examined experimentally. The results of these analyses are provided in Table 1 for all 15 complexes, and representative analyses are shown in Figure 3 for 1-methylimidazole with all three alkali metal ions. A comparable set of figures for the remaining 12 M^+(azole) complexes is available in the Supporting Information as Figure S2. In all cases, the experimental cross sections for reactions 2 are accurately reproduced by a loose PSL TS model.[4] Previous work has shown that this model provides the most accurate assessment of the kinetic shifts for CID processes for electrostatic ion−molecule complexes.[1−9,13−15,55,56] Good reproduction of the data is obtained over energy ranges exceeding 2.5 eV and cross-section magnitudes of at least a factor of 100. Table 1 also includes values of E_0 obtained without including the RRKM lifetime analysis. Comparison of these values with E_0(PSL) values shows that the kinetic shifts observed for these systems vary from 0.01 to 0.43 eV for Li^+, from 0.00 to 0.10 eV for Na^+, and from 0.00 to 0.03 eV for K^+. The total number of vibrational modes varies for these azoles: 21 for pyrazole, 24 for pyrrole, 30 for 1-methylpyrazole and 1-methyimidazole, and 33 for 1-methylpyrrole. This explains

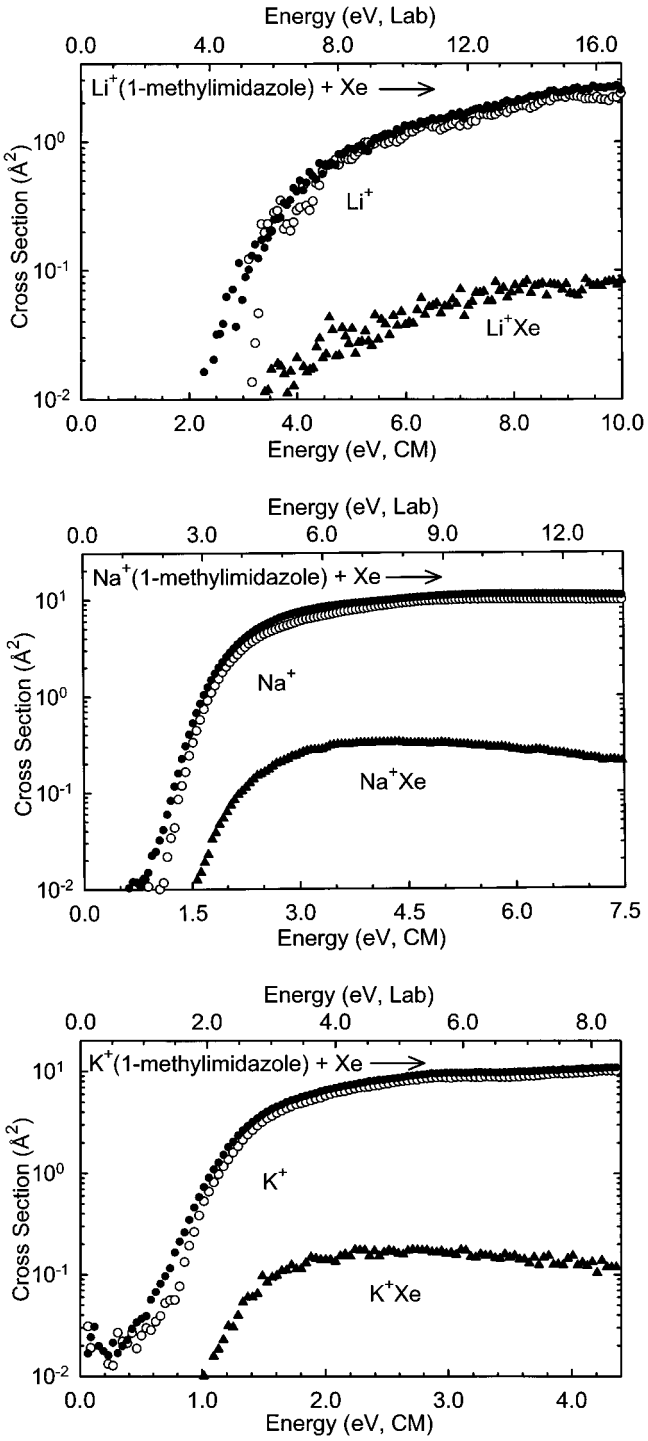

Figure 2. Cross sections for collision-induced dissociation of the M^+-(1-methylimidazole) complexes where $M^+ = Li^+$ (top panel), Na^+ (middle panel), and K^+ (bottom panel), with Xe as a function of kinetic energy in the center-of-mass frame (lower *x*-axis) and the laboratory frame (upper *x*-axis). Data are shown for a xenon pressure of ~0.2 mTorr (●) and extrapolated to zero (○). Cross sections for the ligand exchange process to form M^+Xe are also shown (▲).

TABLE 1: Fitting Parameters of Equation 1, Threshold Dissociation Energies at 0 K, and Entropies of Activation at 1000 K of M^+(azole)[a]

reactant complex	σ_0[b]	n[b]	E_0[c] (eV)	E_0(PSL) (eV)	kinetic shift (eV)	ΔS(PSL) (J mol^{-1} K^{-1})
Li^+(pyrrole)	0.7 (0.2)	1.7 (0.1)	1.85 (0.08)	1.84 (0.17)	0.01	53 (2)
Na^+(pyrrole)	13.3 (1.0)	1.3 (0.1)	1.06 (0.05)	1.06 (0.05)	0.00	44 (2)
K^+(pyrrole)	1.3 (0.1)	2.8 (0.1)	0.87 (0.04)	0.87 (0.04)	0.00	39 (3)
Li^+(1-methylpyrrole)	0.9 (0.1)	1.5 (0.1)	2.06 (0.09)	1.92 (0.17)	0.14	52 (2)
Na^+(1-methylpyrrole)	17.4 (0.6)	1.2 (0.1)	1.16 (0.04)	1.15 (0.04)	0.01	45 (2)
K^+(1-methylpyrrole)	17.3 (1.8)	1.0 (0.1)	0.91 (0.04)	0.91 (0.07)	0.00	41 (2)
Li^+(pyrazole)	0.2 (0.1)	1.8 (0.1)	1.97 (0.06)	1.94 (0.17)	0.03	31 (2)
Na^+(pyrazole)	11.2 (2.3)	1.2 (0.1)	1.33 (0.09)	1.33 (0.09)	0.00	25 (2)
K^+(pyrazole)	19.9 (3.1)	1.0 (0.1)	0.87 (0.03)	0.87 (0.03)	0.00	17 (2)
Li^+(1-methylpyrazole)	4.0 (0.5)	1.5 (0.1)	2.39 (0.14)	2.15 (0.19)	0.24	38 (2)
Na^+(1-methylpyrazole)	13.6 (0.6)	1.2 (0.1)	1.40 (0.03)	1.36 (0.03)	0.04	29 (2)
K^+(1-methylpyrazole)	30.8 (2.5)	1.1 (0.1)	0.99 (0.04)	0.98 (0.04)	0.01	22 (2)
Li^+(1-methylimidazole)	1.2 (0.3)	1.6 (0.1)	2.94 (0.13)	2.51 (0.21)	0.43	32 (2)
Na^+(1-methylimidazole)	13.0 (0.6)	1.2 (0.1)	1.77 (0.05)	1.67 (0.05)	0.10	34 (2)
K^+(1-methylimidazole)	12.6 (0.5)	1.2 (0.1)	1.24 (0.03)	1.21 (0.03)	0.03	19 (2)

[a] Uncertainties are listed in parentheses. [b] Average values for loose PSL transition state. [c] No RRKM analysis.

why the kinetic shifts for pyrrole and pyrazole are smaller than observed for the other azoles. As expected, among the three methyl-substituted azoles (1-methylpyrrole, 1-methylpyrazole, and 1-methylimidazole) that have the same number of heavy atoms and thus lower frequencies, the observed kinetic shifts should correlate directly with the density of states of the complex at threshold, which depends on the measured BDE. Thus the kinetic shifts are largest for 1-methylimidazole followed by 1-methylpyrazole and 1-methylpyrrole, in agreement with the measured BDEs, as shown in Table 1.

The entropy of activation, $\Delta S^{\ddagger}$, is a measure of the looseness of the TS and also a reflection of the complexity of the system. It is largely determined by the molecular parameters used to model the energized molecule and the TS but also depends on the threshold energy. Listed in Table 1, $\Delta S^{\ddagger}$(PSL) values at 1000 K show modest variations, as expected on the basis of the similarity of these systems. The $\Delta S^{\ddagger}$(PSL) values decrease from the Li^+ to Na^+ to K^+ systems and range between 17 and 53 J K^{-1} mol^{-1} across these systems. It is also interesting to note that the complexes that bind via cation$-\pi$ interaction have entropies of activation more than 50% larger than those of the complexes that bind via σ interaction with the nitrogen lone pair of electrons in the plane of the molecule. This seems quite reasonable, as binding of the cation in the π-binding complexes should influence a larger number of vibrational modes. These entropies of activation can be favorably compared to a wide variety of noncovalently bound complexes previously measured in our laboratory and to $\Delta S^{\ddagger}_{1000}$ values in the range of 29$-$46 J mol^{-1} K^{-1} collected by Lifshitz for several simple bond-cleavage dissociations of ions.[65]

Theoretical Results. Theoretical structures for the neutral azoles and for the complexes of these molecules with H^+, Li^+, Na^+, and K^+ were calculated as described above. Details of the final geometries for each of these species are given in the Supporting Information in Table S3. Results of the most stable conformations of all six Na^+(azole) complexes are shown in Figures 4 and 5.[66] The neutral molecules are very nearly planar; deviations from planarity are less than 0.1° in all cases, (with the exception of the hydrogen atoms of the methyl group in the methyl-substituted azoles). Two types of binding geometries are found for the M^+(azole) complexes, π and σ binding. In contrast, only one type of binding geometry is found for the H^+(azole) complexes. As a result of its small size, H^+ is only capable of interacting with one site, and therefore no π-binding geometries are found.

H^+(azole) Complexes. In these complexes the interaction of the proton is quite different for the azoles that do not possess a lone pair of electrons in the plane of the molecule, pyrrole and 1-methylpyrrole, than for the azoles that do, pyrazole, 1-methylpyrazole, imidazole, and 1-methylimidazole. Three distinct binding geometries are found for pyrrole and 1-methylpyrrole: binding to N1, C2, and C3. Binding at any of these sites disrupts the π system and forces the hydrogen atom or methyl group attached to that site out of the plane. Although nitrogen is more electronegative than carbon, the most favorable binding site is at the C2 position. Binding at C2 is favored over binding at C3 by 17.7 and 7.1 kJ/mol, and over binding at N1 by 75.7 and 76.1 kJ/mol for pyrrole and 1-methylpyrrole, respectively. In contrast, only one stable binding site is found for proton binding to pyrazole, 1-methylpyrazole, imidazole, and 1-methylimidazole. In all cases, the proton binds to the lone pair of electrons of the nitrogen atom that lies in the plane of the azole ring. Proton binding to these azoles is stronger than to pyrrole and 1-methylpyrrole, most likely the result of loss of π resonance stabilization in the latter complexes. The distortion of the azole molecule that occurs upon protonation is much more significant for the pyrrole and 1-methylpyrrole complexes than for the other azoles. Bond lengths and angles change in the most extreme cases by less than 0.107 Å and 18.1°, respectively.

***π*-Binding Complexes.** In these complexes the interaction of the alkali metal ion is with the π-electron density of the aromatic ring. Thus, the azole ring acts as a six-electron donor. Although this type of binding is possible for all of the M^+-(azole) complexes examined, it is less favorable than the σ-binding geometry whenever a lone pair of electrons in the plane of the azole molecule is available for binding. Therefore, only pyrrole and 1-methylpyrrole employ π binding in their ground-state geometries. The optimized structures of Na^+-(pyrrole) and Na^+(1-methylpyrrole) are shown in Figure 4. In both cases, the metal ion sits above the ring such that it is displaced from the center of the ring in the direction away from the nitrogen atom as might be expected on the basis of the dipole moment of the pyrrole and 1-methylpyrrole ligands (see Figures 1 and 4). The metal$-$azole ring distance is found to increase with increasing size of the cation as expected. The only other complexes for which stable minima of the π-binding type are

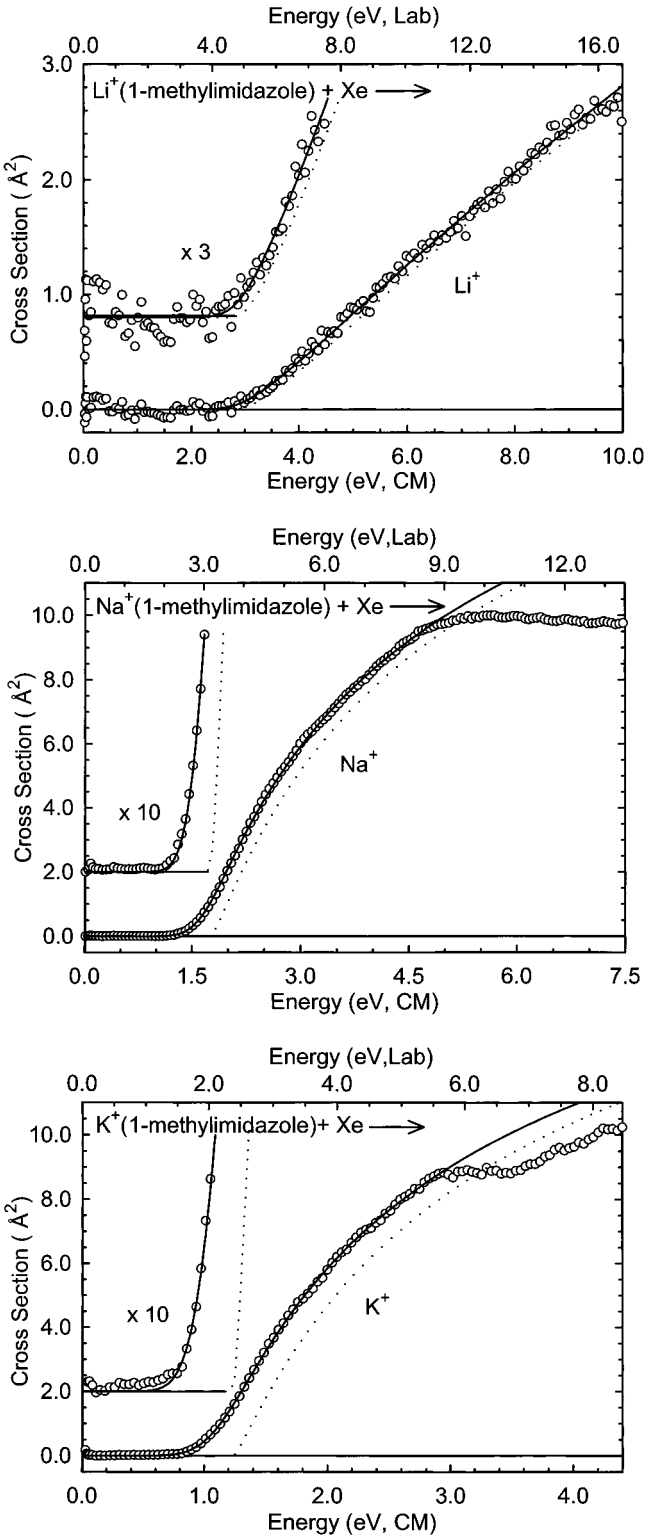

Figure 3. Zero-pressure extrapolated cross section for collision-induced dissociation of the M^+(1-methylimidazole) complexes where M^+ = Li^+ (top panel), Na^+ (middle panel), or K^+ (bottom panel), with Xe in the threshold region as a function of kinetic energy in the center-of-mass frame (lower *x*-axis) and the laboratory frame (upper *x*-axis). Solid lines show the best fits to the data using eq 1 convoluted over the neutral and ion kinetic energy distributions. A dashed line shows the model cross sections in the absence of experimental kinetic energy broadening for reactants with an internal energy corresponding to 0 K.

found are for Li^+(pyrazole), Li^+(1-methylpyrazole), and K^+-(1-methylpyrazole). In these cases, the π-binding geometries are found to be 46.7, 40.5, and 17.1 kJ/mol less stable than the

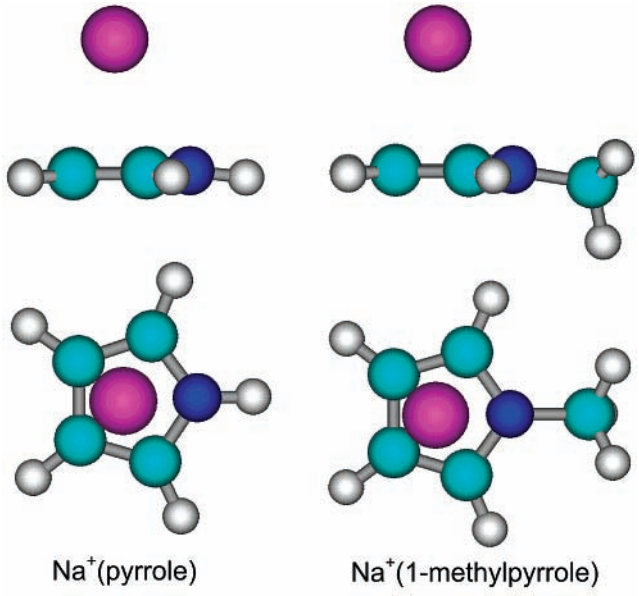

Figure 4. MP2(full)/6-31G* optimized geometries of π-type binding Na^+(azole) complexes, where azole = pyrrole and 1-methylpyrrole. Two views of each optimized structure are shown.

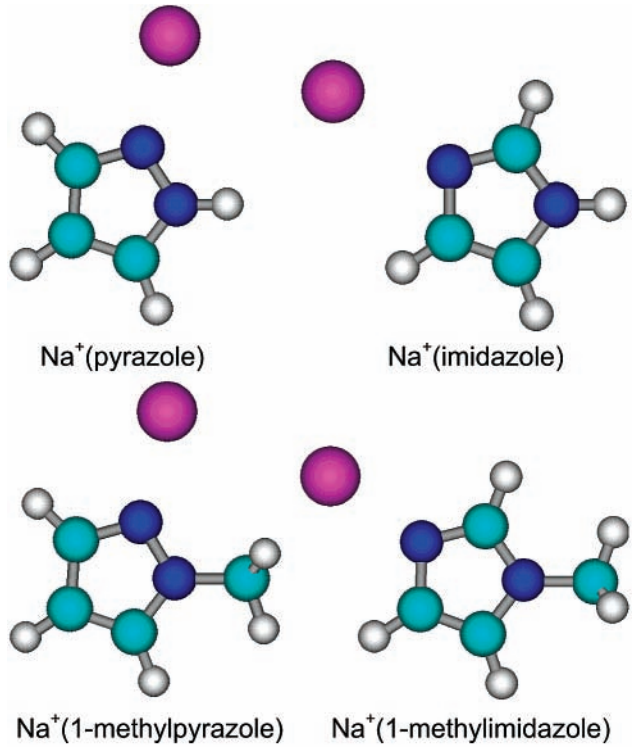

Figure 5. MP2(full)/6-31G* optimized geometries of σ-type binding Na^+(azole) complexes, where azole = pyrazole, 1-methylpyrazole, imidazole, and 1-methylimidazole.

corresponding σ-binding geometries, respectively. The optimized structures of the excited-state conformers of Li^+(pyrazole), Li^+-(1-methylpyrazole), and K^+(1-methylpyrazole) are shown in Figure 6. In the Li^+ complexes, the metal ion sits above the ring but is displaced toward N2, so as to align the metal ion with the direction of the dipole moment (see Figures 1 and 6). It is interesting to note that Li^+ sits closer to the center of the ring in the Li^+(1-methylpyrazole) complex than in the Li^+-(pyrazole) complex even though these molecules have very similar dipole moments. In addition, Li^+ sits closer to the plane of the azole ligand in the Li^+(1-methylpyrazole) complex than

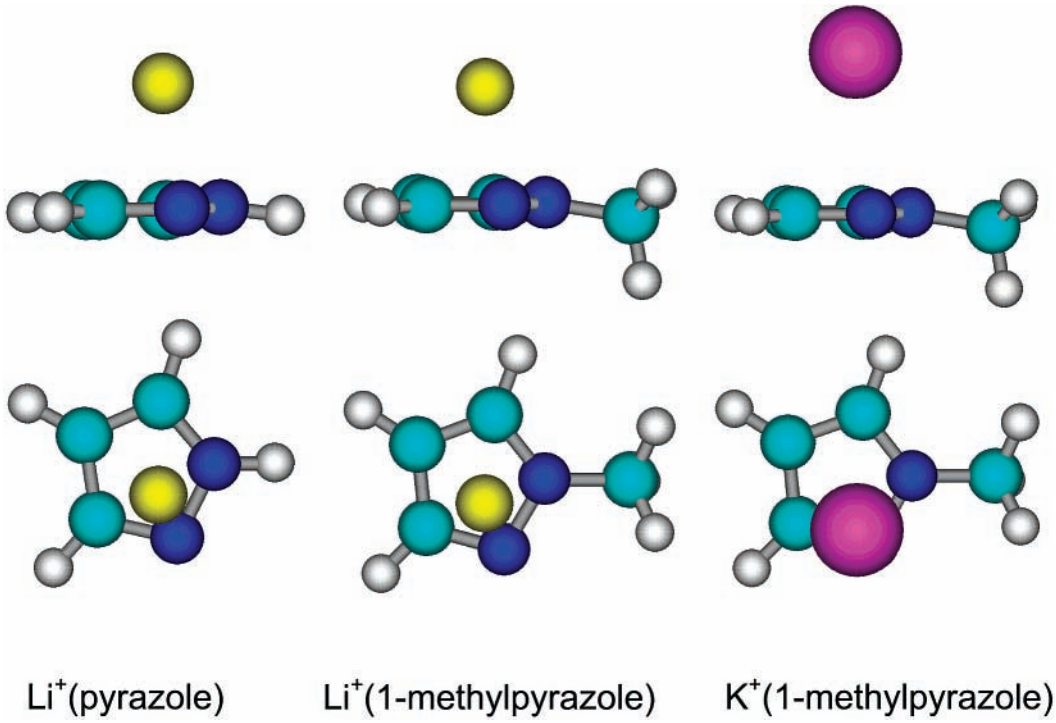

Figure 6. MP2(full)/6-31G* optimized geometries of π-type binding of the Li^+(pyrazole), Li^+(1-methylpyrazole), and K^+(1-methylpyrazole) complexes.

in the Li^+(pyrazole) complex. In fact the Li^+−ring and Li^+−N distances differ by less than 0.001 Å in the π- and σ-binding geometries of Li^+(1-methylpyrazole) complexes. In contrast, these distances differ by 0.037 Å in the Li^+(pyrazole) complexes and strongly favor the σ-binding geometry. The inductive effects of the methyl group result in an increase in the binding strength for both binding geometries. However, the increased stability is greater for the π-binding geometry (14.2 kJ/mol) than the σ-binding geometry (8.0 kJ/mol). In the K^+(1-methylpyrazole) complex, K^+ sits more directly above N2 than is observed for the corresponding Li^+ complex, and as found for the other cation−π complexes the metal−azole ring distance is larger. In all other cases, the starting π-binding complex always converged to the more energetically favorable σ-binding complex. From this we concluded that the potential energy surfaces for these M^+(azole) complexes have very shallow minima associated with the π-binding geometries that the geometry optimization procedure easily finds its way out of. In hopes of finding the local minima associated with the π-binding geometries, we made multiple attempts to optimize all of the M^+(azole) π-binding complexes while severely restricting the step size (magnitude of bond length and bond angle changes) in each step of the optimization procedure. Unfortunately this causes the geometry optimization to become significantly more time-consuming. However, it was only through this procedure that we were able to find the π-binding complexes of Li^+(pyrazole) and K^+(1-methylpyrazole). It seems odd that all of our attempts to find a π-binding complex for Na^+(1-methylpyrazole) eventually converged to the σ-binding geometry when we were able to find them for the Li^+(1-methylpyrazole) and K^+(1-methylpyrazole) complexes. Surely, the Na^+ complex is more strongly bound and the minima should be deeper than for the K^+ complex. Thus the ability to find the local π-binding minima for these M^+(azole) complexes is extremely sensitive to the initial starting geometry. In all cases for which a π-binding complex could be found, the distortion of the azole molecule that occurs upon complexation to the alkali metal cation is minor. The change in geometry is largest for the Li^+ systems and decreases with increasing size of the cation. Bond lengths and angles change in the most extreme cases by less than 0.020 Å and 0.6°, respectively. It is interesting to note that the effect of cation binding is felt almost equally by all atoms of the ring such that all of the bond lengths within the ring are nearly equally affected. In addition, slightly larger distortions of the azole ligand occur for the complexes to the methyl-substituted azoles than to the corresponding unsubstituted azoles as a result of the shorter cation−ligand distances and therefore stronger binding.

***σ*-Binding Complexes.** As discussed above, the M^+(azole) complexes favor σ-binding geometries whenever a lone pair of electrons in the plane of the azole molecule is available for binding. Thus, the ground-state geometries for the complexes to pyrazole, 1-methylpyrazole, imidazole, and 1-methylimidazole all involve σ binding of the alkali metal cation to the lone pair of electrons on a nitrogen atom. Again, the distortion of the azole molecule that occurs upon complexation to the alkali metal cation is minor. The change in geometry is largest for the Li^+ systems and decreases with increasing size of the cation. Bond lengths and angles change in the most extreme cases by less than 0.017 Å and 1.9°, respectively. In contrast to that observed for the π-binding complexes, the distortion of the azole ring is asymmetric with the bond lengths and angles closest to the binding site more profoundly affected by the binding than sites distant from the metal ion. Again, very slightly larger distortions of the azole ligand occur for the complexes to 1-methylpyrazole and 1-methylimidazole than to pyrazole and imidazole, respectively. This again is likely a result of the shorter cation−ligand distance and therefore stronger binding in the methyl-substituted azoles.

Conversion from 0 to 298 K. To allow comparison to previous literature values[6,31,32,34] and commonly used experimental conditions, we convert the 0 K bond energies determined here (experimentally and theoretically) to 298 K bond enthalpies and free energies. The enthalpy and entropy conversions are

TABLE 2: Enthalpies and Free Energies of Transition Metal Ion Binding to Azoles at 298 K[a]

reactant complex	ΔH_0[b]	ΔH_0[c]	$\Delta H_{298} - \Delta H$[c]	ΔH_{298}	ΔH_{298}[c]	$T\Delta S_{298}$[c]	ΔG_{298}	ΔG_{298}[c]
H^+(pyrrole)	869.2 (16.0)	836.9	6.2 (0.1)	875.4 (16.0)[e]	843.1	25.9 (0.1)	849.5 (16.0)	817.2
Li^+(pyrrole)	177.4 (16.6)	158.1	3.6 (2.1)	181.1 (16.7)	161.7	34.0 (4.6)	147.1 (17.4)	127.7
Na^+(pyrrole)	101.8 (4.8)	102.0	1.9 (1.6)	103.7 (4.8)	103.9	34.5 (5.4)	69.2 (7.4)	69.3
K^+(pyrrole)	83.7 (3.6)	80.7	1.4 (1.5)	85.1 (3.6)	82.1	30.5 (5.5)	54.6 (6.8)	51.6
H^+(1-methylpyrrole)	–	859.2	6.6 (0.1)	–	865.8	27.4 (0.1)	–	838.4
Li^+(1-methylpyrrole)	186.2 (16.8)	171.6	3.6 (2.1)	189.8 (16.9)	175.2	35.0 (4.7)	154.8 (17.6)	140.2
Na^+(1-methylpyrrole)	111.3 (3.4)	111.2	1.8 (1.6)	113.1 (3.4)	113.0	32.3 (5.4)	80.8 (6.6)	80.7
K^+(1-methylpyrrole)	87.8 (6.3)	88.4	1.3 (1.4)	89.1 (6.3)	89.7	31.2 (5.6)	57.9 (8.6)	58.5
H^+(pyrazole)	888.5 (16.0)	866.1	5.6 (0.1)	894.1 (16.0)[e]	871.7	25.8 (0.1)	868.3 (16.0)	845.9
Li^+(pyrazole)	187.1 (16.1)	171.0	2.1 (1.7)	189.2 (16.2)	173.1	29.7 (5.0)	159.5 (16.9)	143.4
Na^+(pyrazole)	128.1 (8.5)	117.7	0.9 (1.4)	129.0 (8.5)	118.6	27.9 (5.6)	101.1 (10.3)	90.7
K^+(pyrazole)	83.8 (3.3)	86.3	0.4 (1.2)	84.2 (3.3)	86.7	26.2 (5.7)	58.0 (6.7)	60.5
H^+(1-methylpyrazole)	906.2 (16.0)	888.0	5.8 (0.1)	912.0 (16.0)[e]	893.8	26.6 (0.1)	885.4 (16.0)	867.2
Li^+(1-methylpyrazole)	207.2 (18.4)	179.0	2.2 (1.7)	209.4 (18.5)	181.2	30.8 (5.0)	178.8 (19.1)	150.4
Na^+(1-methylpyrazole)	131.5 (2.9)	123.4	0.9 (1.3)	132.4 (2.9)	123.3	28.8 (5.6)	103.6 (6.4)	95.5
K^+(1-methylpyrazole)	94.3 (3.6)	90.8	0.5 (1.1)	94.8 (3.6)	91.3	27.1 (5.7)	67.7 (6.9)	64.2
H^+(imidazole)	936.6 (16.0)	922.2	6.2 (0.1)	942.8 (16.0)[e]	928.4	26.2 (0.1)	916.6 (16.0)	902.2
Li^+(imidazole)	210.8 (9.5)[d]	202.7	2.4 (1.7)	213.2 (9.7)	205.1	28.0 (3.2)	185.2 (10.2)	177.1
Na^+(imidazole)	139.7 (5.2)[d]	144.5	1.2 (1.2)	140.9 (5.3)	145.7	27.6 (4.1)	113.3 (6.7)	118.1
K^+(imidazole)	109.0 (5.6)[d]	108.6	0.7 (1.2)	109.7 (5.7)	109.3	26.2 (4.5)	83.5 (7.3)	83.1
H^+(1-methylimidazole)	953.5 (16.0)	943.1	6.1 (0.1)	959.6 (16.0)[e]	949.2	26.7 (0.1)	932.9 (16.0)	922.5
Li^+(1-methylimidazole)	242.3 (20.2)	214.4	2.3 (1.7)	244.6 (20.3)	216.7	30.9 (5.0)	213.7 (20.9)	185.8
Na^+(1-methylimidazole)	160.8 (5.0)	154.1	1.0 (1.4)	161.8 (5.0)	155.1	29.2 (5.6)	132.6 (7.6)	126.0
K^+(1-methylimidazole)	117.2 (2.7)	116.7	0.5 (1.1)	117.7 (2.7)	117.2	27.2 (5.7)	90.5 (6.4)	90.0

[a] Values are given in kJ/mol; uncertainties are listed in parentheses. [b] Values taken from Table 3. [c] Ab initio values from calculations at the MP2(full)6-311+G(2d,2p)//MP2(full)/6−31G* level of theory with all frequencies scaled by 0.9646. [d] Values taken from Rodgers and Armentrout.[6] [e] See NIST Webbook.[33]

calculated using standard formulas (assuming harmonic oscillator and rigid rotor models) and the vibrational and rotational constants determined for the MP2(full)/6-31G* optimized geometries, which are given in Tables S1 and S2. Table 2 lists the 0 and 298 K enthalpy, free energy, and enthalpic and entropic corrections for all systems experimentally and theoretically determined (from Tables 1 and 3). Uncertainties in the enthalpic and entropic corrections are determined by 10% variation in the molecular constants. For the metal complexes where the metal−ligand frequencies are very low and may not be adequately described by theory, the listed uncertainties also include changing the three frequencies associated with the metal−azole interaction by a factor of 2. The latter provides a conservative estimate of the computational errors in these low-frequency modes and is the dominant source of the uncertainties listed.

In addition, we have adjusted the free energy values at 373 K for the complexes of Li^+ to pyrazole, 1-methylpyrazole, imidazole, and 1-methylimidazole taken from the work of Taft and co-workers[31,32] to 0 K BDEs for comparison to the results obtained here. The 373 K free energies reported for these systems are 140.6, 143.5, 159.8, and 168.2 kJ/mol. The uncertainties in these free energy values reflect the uncertainty of the anchor used, $Li^+(H_2O)$ (8.0 kJ/mol), taken from work of Rodgers and Armentrout.[5] The conversion values required here are $T\Delta S_{373}$ and $\Delta H_{373} - \Delta H_0$, which were calculated for each system individually. The resultant values are compared to the present results in Table 3 and Figure 7 and are discussed further below. We have also adjusted the 298 K proton affinities of the azoles taken from the NIST webbook compilation to 0 K for comparison to the values calculated here.[33] Thermal corrections for the protonated systems are also provided in Table 2.

Discussion

Comparison of Theory and Experiment. The metal cation affinities of pyrrole, 1-methylpyrrole, pyrazole, 1-methylpyrazole, and 1-methylimidazole at 0 K measured here by guided ion beam mass spectrometry are summarized in Table 3. Also listed here are the 0 K BDEs calculated at the MP2(full)/6-311+G(2d,2p)//MP2(full)6-31G* level including full MP2 correlation, zero-point energy corrections, and basis-set superposition error corrections.[61,67,68] The calculations performed here also include the analogous H^+(azole) and M^+(imidazole) complexes. Experimental results for the H^+(azole)[33] and M^+(azole)[6,31,32] systems taken from previous studies are also listed in Table 3 for comparison. The agreement between theory and experiment for the M^+(azole) complexes is illustrated in Figure 7. It can be seen that the agreement is very good over the nearly 160 kJ/mol variation in binding affinities measured here. For the 15 M^+(azole) systems examined experimentally, the mean absolute deviation (MAD) between theory and experiment is 9.4 ± 9.7 kJ/mol. This is slightly larger than the average experimental error of 8.8 ± 6.7 kJ/mol. However, more careful inspection of the data makes it clear that the Li^+ complexes are the principal contributors to the deviations. For the five Li^+ systems, the MAD is 21.2 ± 6.5 kJ/mol, whereas the Na^+ and K^+ systems combined have a MAD of 3.6 ± 3.7 kJ/mol. The poorer agreement for the Li^+ systems may result from the experimental difficulty in measuring cross sections for Li^+ as a result of the difficulty associated with efficient detection of low mass ions as discussed in the Experimental Section. An alternative explanation was proposed in an earlier study,[1] where it was also observed that theory systematically underestimates the bond energies for the Li^+ complexes, which may be a result of the higher degree of covalency in the metal−ligand bond (see discussion below). The additional covalency of the metal−azole bonds in the Li^+ systems compared to those for Na^+ and K^+ suggests that this level of theory may be inadequate for a complete description of the former systems. Support for this conclusion comes from comparison of the theoretical and experimental values for the protonated azoles, which possess an even higher degree of covalency than the Li^+ complexes. The MAD for the five protonated azoles previously examined

TABLE 3: Experimental and Calculated Enthalpies of Proton and Alkali Metal Ion Binding to Azoles at 0 K

complex	binding geometry	experiment		theory		
		GIBMS[a]	literature	D_e[b]	D_0[c]	$D_{0,BSSE}$[d]
H^+(pyrrole)	N1			803.8	769.9	761.2
	C2		869.2 (16.0)[e]	879.4	845.2	836.9
	C3			858.8	827.0	819.2
Li^+(pyrrole)	π	177.4 (16.6)		175.1	167.3	158.1
Na^+(pyrrole)	π	101.8 (4.8)		115.7	111.1	102.0
K^+(pyrrole)	π	83.7 (3.6)		89.6	85.9	80.7
H^+(1-methylpyrrole)	N1			827.6	792.8	783.1
	C2			900.6	867.5	859.2
	C3			891.3	859.6	851.8
Li^+(1-methylpyrrole)	π	186.2 (16.8)		189.0	181.2	171.6
Na^+(1-methylpyrrole)	π	111.3 (3.6)		125.2	120.9	111.2
K^+(1-methylpyrrole)	π	87.8 (6.3)		97.4	94.0	88.4
H^+(pyrazole)	σ		888.5 (16.0)[e]	909.5	875.7	866.1
Li^+(pyrazole)	σ	187.1 (16.1)	172.5 (9.5)[f]	182.9	177.1	171.0
	π			137.7	132.6	124.3
Na^+(pyrazole)	σ	128.1 (8.5)		127.6	124.2	117.7
K^+(pyrazole)	σ	83.8 (3.3)		92.8	90.1	86.3
H^+(1-methylpyrazole)	σ		906.2 (16.0)[e]	932.1	897.9	888.0
Li^+(1-methylpyrazole)	σ	207.2 (18.4)	176.5 (9.5)[f]	191.1	185.3	179.0
	π			153.0	147.5	138.5
Na^+(1-methylpyrazole)	σ	131.5 (2.9)		133.6	130.2	123.4
K^+(1-methylpyrazole)	σ	94.3 (3.6)		97.5	94.9	90.8
	π			81.1	78.9	73.7
H^+(imidazole)	σ		936.6 (16.0)[e]	967.9	931.9	922.2
Li^+(imidazole)	σ	210.8 (9.5)[g]	187.6 (9.5)[f]	215.5	208.7	202.7
Na^+(imidazole)	σ	139.7 (5.2)[g]		155.1	150.8	144.5
K^+(imidazole)	σ	109.0 (5.6)[f]		115.6	112.3	108.6
H^+(1-methylimidazole)	σ		953.5 (16.0)[e]	988.3	952.8	943.1
Li^+(1-methylimidazole)	σ	242.3 (20.2)	201.4 (9.5)[f]	226.8	220.3	214.4
Na^+(1-methylimidazole)	σ	160.8 (5.0)		164.5	160.5	154.1
K^+(1-methylimidazole)	σ	117.2 (2.7)		123.5	120.5	116.7

[a] Present results, threshold collision-induced dissociation, given in kJ/mol. [b] Calculated at the MP2(full)/6-311+G(2p,2d) level of theory using the MP2(full)/6-31G* optimized geometries. [c] Including zero-point energy corrections with frequencies scaled by 0.9646. [d] Also includes basis-set superposition error corrections. [e] See NIST Webbook. Adjusted to 0 K.[33] [f] See Taft and co-workers.[31,32] Values are adjusted to 0 K. [g] See Rodgers and Armentrout.[6]

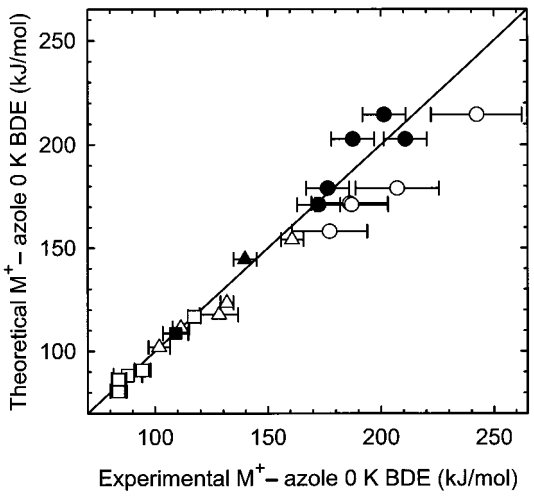

Figure 7. Theoretical versus experimental bond dissociation energies at 0 K (in kJ/mol) of M^+(azole), where $M^+ = Li^+$ (○), Na^+ (△), and K^+ (□) and azole = pyrrole, 1-methylpyrrole, pyrazole, 1-methylpyrazole, imidazole, and 1-methylimidazole. Experimental results include values taken from Rodgers and Armentrout[6] and Taft and co-workers,[31,32] adjusted to 0 K, where $M^+ = Li^+$ (●), Na^+ (▲), and K^+ (■).

is 19.5 ± 8.4 kJ/mol, very similar to that found for the Li^+ complexes. However, it is also possible that the additional covalency means that the PSL model used to describe the TS for dissociation may not provide an adequate description of the Li^+ complexes. If a tighter transition state is appropriate, larger kinetic shifts would be expected for these systems. This would result in lower threshold values and better agreement with theory. For the Na^+ and K^+ systems, the kinetic shifts are much smaller and the metal−azole bonds more electrostatic, such that the treatment here is definitely appropriate and would not change greatly with different assumptions about the TS.

Comparison with Literature Values. Table 3 and Figure 7 also compare the present experimental results to those of Taft and co-workers, who used ion cyclotron resonance mass spectrometry to measure lithium ion transfer equilibria between reference species and pyrazole, 1-methylpyrazole, imidazole, and 1-methylimidazole.[31,32] Recently, Rodgers and Armentrout[3] have noted that the anchoring process used by Taft et al.[31] was flawed, a conclusion that has been substantiated by work of Burk et al.[32] In this latter work, the early results of Taft et al. have been revised and placed on an absolute scale using the bond energy for $Li^+(H_2O)$ taken from Rodgers and Armentrout.[2] This agrees well with a revised value published subsequently[5] but with a smaller uncertainty of 8.0 kJ/mol. We assign this latter value as the absolute uncertainty of the Li^+ basicity scale given by Burk et al. and then adjust their values for Li^+(pyrazole), Li^+(1-methylpyrazole), Li^+(imidazole), and Li^+(1-methylimidazole) to 0 K as discussed above. The resulting values are 14.6, 30.7, 23.2, and 40.9 kJ/mol lower than that measured here, respectively. However, their adjusted values are in good agreement with theory for pyrazole (MAD = 1.5 kJ/mol) and 1-methylpyrazole (MAD = 2.5 kJ/mol) but are

systematically lower than theory for imidazole (MAD = 15.1 kJ/mol) and 1-methylimidazole (MAD = 13.0 kJ/mol). This discrepancy might suggest that the across-the-board reduction of the free energies of Li^+ binding reported by Taft et al.[31] suggested in our earlier work[2] and supported by the work of Burk et al.[32] may only be appropriate for a subset of the systems in the original study. In any event, comparison with theory and Taft's results suggests that the values measured here for the Li^+ systems appear to be too high.

Previous theoretical calculations to determine the alkali metal ion affinities have been reported for Na^+ binding to pyrrole[34] and imidazole.[6,8,35,36] In a combined experimental and theoretical study of the binding energies of gas-phase metal ions with pyrrole, Dunbar and co-workers[34] reported a theoretical binding energy for Na^+(pyrrole) of 107.9 kJ/mol. This value was determined from density functional theory calculations with the B3LYP functional in which a basis set consisting of the 6-311+G* basis was used for the Na^+ ion and the 6-31G* basis for the C, N, and H atoms for geometry optimization and frequency analysis. To improve the accuracy of the calculated binding energy, additional diffuse functions for the C and N atoms were added using the 6-31+G* basis set. Their calculated value is 5.9 kJ/mol higher than that calculated here. These results are consistent with earlier work establishing an absolute sodium ion affinity scale,[8] in which MP2 values consistently showed better agreement to experimental values (both threshold CID and high-pressure mass spectrometry) than B3LYP values. It is also consistent with the observation that the B3LYP values tend to be somewhat high for monoligated Na^+(ligand) complexes.

Theoretical calculations to determine the binding energy of Na^+(imidazole) have been reported in several studies.[6,8,35,36] In earlier work Rodgers and Armentrout performed a study similar to that carried out here to measure the alkali metal ion affinities of several azoles not examined in the present study, (imidazole, 1,2,3-triazole, 1,2,4-triaziole, and tetrazole).[6] Their interest had been to characterize the tautomeric form of the azole accessed in the experiment. To accomplish this, theoretical calculations were performed for both tautomeric forms and the measured BDEs compared to the theoretical BDEs to establish whether tautomerization occurred during complex formation or CID. Imidazole had been included in the study as it has only one tautomeric form and thus would provide an absolute measure of the accuracy of the theory employed. As this work was performed several years ago, the level of theory employed, MP2/6-31G*//HF/6-31G*, was lower than that employed here. The value for the BDE of Na^+(imidazole) they calculated was 165.1 kJ/mol, 25.4 kJ/mol greater than the measured value and 20.6 kJ/mol higher than that calculated here. Thus it is obvious that the level of theory employed here is significantly more accurate. Indeed in later studies by Armentrout and Rodgers[8] and Ohanessian and co-workers[35,36] to establish an absolute sodium cation affinity scale, calculations at the level employed here, MP2(full)/6-311+G(2d,2p)//MP2(full)/6-31G*, were shown to yield reasonably accurate sodium cation affinities at modest computational cost. In these studies, the calculated BDE of Na^+-(imidazole) is consistent with the value calculated here.

Trends in the Binding of Alkali Metal Ions to the Azoles. It has previously been established that both electrostatic and inductive interactions are the dominant interactions responsible for the strength of binding of alkali metal ions to neutral ligands. Therefore, trends in the binding energies of such metal−ligand complexes can often be understood by correlating the binding affinity with size of the metal ion, nature of the binding interaction (σ vs π binding), dipole moment, quadrupole moment, and polarizability of the ligand.

Size of the Metal Ion. As has been found in earlier studies, the size of the metal ion is the most influential factor determining the strength of the binding interaction in these systems. In the M^+(azole) systems examined here, the binding strength varies with the metal ion such that Li^+ binds ∼59% more strongly than Na^+, which in turn binds ∼36% strongly than K^+. These ratios are somewhat smaller for the theoretical binding strength, which finds that Li^+ binds ∼47% more strongly than Na^+, which in turn bind ∼32% more strongly than K^+. Because these complexes are largely electrostatic in nature, this trend is easily understood on the basis of size of the metal ion. Smaller metal ions lead to stronger ion-dipole, ion-induced dipole, and ion-quadrupole interactions in these systems because the metal−ligand bond distances are smaller.

Theoretical calculations indicate that the charge retained on the metal ion is fairly similar from one M^+(azole) complex to another and follows the order Li^+ (∼0.7−0.8e) < Na^+ (∼0.92e) < K^+ (∼0.98e).[69] These results confirm the electrostatic nature of the bonding but also demonstrate that there is some covalency in the metal−ligand interaction, particularly for the Li^+ systems. The shorter bond distance in the complexes to the smaller cations allow the metal ion to more effectively withdraw electron density from the neutral ligand, reducing the charge retained on the metal ion and increasing the covalency of the metal−ligand interaction.

***σ* versus *π* Interactions.** The nature of the binding interaction can also exert a very strong influence on the binding strength of metal−ligand complexes. As mentioned above, two types of binding geometries are found for the M^+(azole) complexes, π and σ binding. In π-binding complexes, the interaction of the alkali metal ion is with the π-electron density of the aromatic ring. Thus, the azole ring acts as a six-electron donor. In the σ-binding complexes, the alkali metal ion interacts with the nitrogen lone pair of electrons in the plane of the azole ring. For covalent bonds it is well established that σ-bonds are stronger than π-bonds. This is because the shared electron density in a σ-bond is largely localized between the two atoms involved in the bond, whereas it spread out over a larger region in a π-bond. This difference in the sharing of electron density makes a typical π-bond only about ∼60% as strong as a typical σ-bond. Similar findings might be expected for noncovalent interactions; however, aromatic systems such as the azoles examined here can act as six-electron donors and thus might be expected to form fairly strong π-binding interactions. Comparison of the BDEs of the π-binding complexes (pyrrole and 1-methylpyrrole) to those measured for σ-binding complexes (pyrazole, 1-methylpyrazole, imidazole, and 1-methylimidazole) shows that indeed the π-binding complexes are less strongly bound than the σ-binding complexes. However, the relative binding affinities for the π-binding complexes are much greater than expected for a typical π-bond, which is likely the result of the azole acting as a six-electron donor. A more quantitative assessment of the relative strength of π vs σ binding is difficult for these systems, as other effects such as the dipole moment and polarizability come into play. However, we can use the theoretical values obtained for the Li^+(pyrazole), Li^+(1-methylpyrazole), and K^+(1-methylpyrazole) complexes for this comparison. The BDE for the π-binding complexes are calculated to be 46.7, 40.5, and 17.1 kJ/mol weaker than the corresponding σ-binding complexes. Thus the strength of the interactions in the π-binding complexes is only 73%, 77%, and 81% as strong as the σ-binding complexes. This is again larger

than typical of a π-bond and is likely the result of pyrazole acting as a six-electron donor. It should also be noted that the calculated BDEs for the π-binding complex of Li^+(pyrazole), Li^+(1-methylpyrazole), and K^+(1-methylpyrazole) are significantly weaker than those found for Li^+(pyrrole), Li^+(1-methylpyrrole), and K^+(1-methylpyrrole), respectively. The presence of the second N atom in the ring decreases the electron density of the aromatic π-system, the polarizability, and the quadrupole moment of the ligand and thus weakens the bond.

Cation$-\pi$ Interaction. As mentioned in the Introduction, the azoles are members of the class of five-membered heteroaromatic compounds referred to as π-excessive N-heterocycles.[16] They are generally thought of in this way because six π-electrons are distributed over five atoms. Thus the π-electron density per atom is 6/5 or 1.2. In comparison to benzene, which shares six π-electrons over six atoms resulting in a π-electron density of 1.0, the azoles represent π-excessive aromatic compounds. However, such an analysis of the π character of the azoles is too simple and really only accurate for pyrrole and its derivatives. This can be seen by comparing the cation$-\pi$ binding energies for the simple azoles to those of benzene[8,37] and those of the methyl-substituted azoles to those of toluene.[38] The measured M^+-pyrrole BDEs are greater than the measured M^+-benzene BDEs by 16.3, 9.2 (13.5), and 10.4 kJ/mol for Li^+, Na^+, and K^+. The calculated M^+-pyrrole BDEs are greater than the calculated M^+-benzene BDEs by 14.8, 2.6, and 3.7 kJ/mol for Li^+, Na^+, and K^+. The measured M^+-1-methylpyrrole BDEs are greater than the measured M^+-toluene BDEs by 3.1 and 7.9 kJ/mol for Li^+ and K^+ but 1.0 kJ/mol less for Na^+. The calculated M^+-1-methylpyrrole BDEs are greater than the calculated M^+-toluene BDEs by 15.8, 12.9, and 10.8 kJ/mol for Li^+, Na^+, and K^+. Thus, pyrrole and 1-methylpyrrole are stronger π-donors than benzene and toluene. Therefore, it seems appropriate to think of pyrrole and 1-methylpyrrole as π-excessive aromatic compounds. In contrast, the calculated Li^+-pyrazole, Li^+-1-methylpyrazole, and K^+-1-methylpyrazole BDEs are less than the calculated Li^+-benzene, Li^+-toluene, and K^+-toluene BDEs by 19.0, 17.3, and 3.9 kJ/mol, respectively. The presence of the second nitrogen atom in the ring withdraws electron density from the π-cloud, weakening the cation$-\pi$ interaction. Thus, pyrazole and 1-methylpyrazole are weaker π-donors than benzene and toluene. Therefore, its seems inappropriate to think of pyrazole and 1-methylpyrazole as π-excessive aromatic compounds. Although we were unable to find local π-minima for any of the M^+(imidazole) and M^+-(1-methylimidazole) complexes, the σ interaction is stronger for these complexes than for the analogous M^+(pyrazole) and M^+-(1-methylpyrazole) complexes. Therefore, it is anticipated that if such minima do exist, they would be weaker π-donors as a consequence of the stronger σ interaction. This will be clearer upon examination of the quadrupole moments of these azoles as discussed below. Again, it seems inappropriate to think of imidazole and 1-methylimidazole as π-excessive aromatic compounds.

Effect of Methyl Substituent. The effect of the methyl substituent on the binding strength can be examined by comparing the methyl-substituted to the unsubstituted azole molecules. As can be seen in Figure 1, the methyl substituent leads to a small increase in the dipole moment, and a modest increase in the polarizability, for each of the azole molecules. The methyl substituent also leads to an increase in the quadrupole moment of the molecule. These three effects should act in concert to increase the binding affinity. Indeed, an increase in the binding affinity is observed upon methyl substitution for all three azoles binding to all three alkali metal ions (see Table 3). The experimental trends are not quite as systematic as that found for the theoretical values, but in general the increase in binding affinity is largest for the Li^+ complexes and smallest for the K^+ complexes. The experimental values suggest that the increase is slightly larger for the σ-binding complexes than the π-binding complexes, whereas the theoretical values suggest the converse is true. In any event, the addition of the methyl substituent acts to increase the dipole moment, polarizability, and quadrupole moment of all three azoles and their binding affinities to all three metal ions.

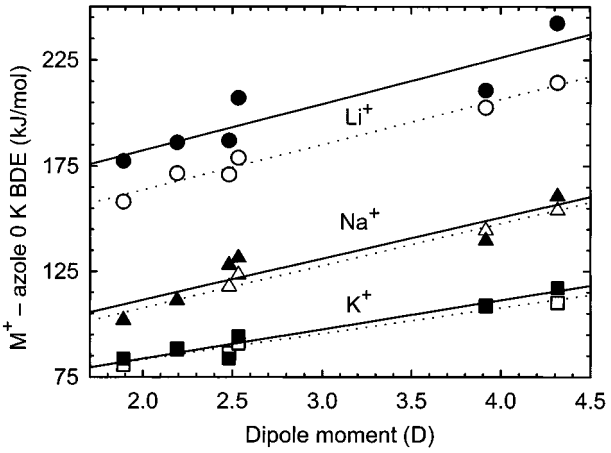

Figure 8. Bond dissociation energies at 0 K of M^+(azole) (in kJ/mol) versus dipole moment of the neutral azole (in D), where $M^+ = Li^+$ (●, ○), Na^+ (▲, △), and K^+ (■, □), and azole = pyrrole, 1-methylpyrrole, pyrazole, 1-methylpyrazole, imidazole, and 1-methylimidazole. Experimental values are indicated with solid symbols, whereas theoretical values are indicated with open symbols. Linear regression analyses of the experimental values are indicated with solid lines; whereas theoretical values are indicated with dotted lines. Experimental values for imidazole are taken from Rodgers and Armentrout.[6]

Influence of Dipole Moment. The influence of the dipole moment of the ligand was alluded to above in the discussion of the effect of methyl substitution. That is, an increase in the binding affinity is expected as the dipole moment of the ligand increases. However, the discussion above was limited to comparing the dipole moments of the methyl-substituted and unsubstituted azoles but does not examine cross comparisons. As seen in Figure 1, the dipole moment of these systems follows the order pyrrole < 1-methylpyrrole < pyrazole < 1-methylpyrazole < imidazole <1-methylimidazole, in agreement with the observed trend in the measured and calculated BDEs. Shown in Figure 8 is the correlation of both the theoretical and experimental BDEs of the 18 M^+(azoles) complexes examined here and the dipole moment of the azole ligand. As can be seen in the figure, the correlation between the calculated BDEs and dipole moments is quite good across all of the azoles examined. A similar correlation is found for the experimental values. However, the deviations from linearity are slightly more pronounced. It is interesting to note that although the nature of the binding is different in the pyrrole and 1-methylpyrrole complexes (π binding vs σ binding for the remaining azoles), good correlation between the binding affinities and the dipole moment is still found.

Influence of Quadrupole Moment. Examination of the influence of the quadrupole moment of the ligand might also provide insight into the observed trends in the alkali metal ion binding affinities of the azoles. However, binding is highly directional and therefore it would be more appropriate to examine the magnitude of the quadrupole moment tensor in the

direction of the binding. The magnitudes of the quadrupole moment tensor in the direction perpendicular to the plane of the azole ring of pyrrole, pyrazole, imidazole, 1-methylpyrrole, 1-methylpyrazole, and 1-methylimidazole are 35.1, 33.0, 32.9, 41.2, 39.0, and 38.9 D Å, respectively. Thus the unsubstituted azoles have similar magnitudes of the quadrupole moment tensor in the π direction, with pyrrole having the largest value and pyrazole and imidazole having nearly equal values. Likewise, the methyl-substituted azoles also have similar moments in the π direction, with 1-methylpyrrole having the largest value and 1-methylpyrazole and 1-methylimidazole having nearly equal values. The relative magnitudes of the quadrupole moment tensor in the π direction suggest that pyrrole should be a stronger π-binding ligand than pyrazole, in agreement with the theoretical binding energies of the cation$-\pi$ complexes. Likewise, 1-methylpyrrole should be a stronger π-binding ligand than 1-methylpyrazole, in agreement with the calculated binding energies of the cation$-\pi$ complexes. Finally, the methyl-substituted azoles should be stronger π-binding ligands than the unsubstituted azoles, in agreement with the theoretical binding energies of these cation$-\pi$ complexes. However, cross comparisons are not as simple: 1-methylpyrazole is found to be a weaker π-binding ligand than pyrrole despite this ligand having a larger magnitude of the quadrupole moment tensor in the π direction. Although no stable local minima of the π-binding type could be found for imidazole and 1-methylimidazole, the magnitude of moments in the π direction for these ligands suggests that if such minima do exist, these complexes should form slightly weaker cation$-\pi$ complexes than pyrazole and 1-methylpyrazole, respectively. Overall, it appears that larger moments lead to stronger binding, particularly for cation$-\pi$ complexes; however, no simple correlation is found that holds across all of these azole systems.

Influence of Polarizability. The polarizabilities of the azole ligands are shown in Figure 1. The polarizabilities follow the order 1-methylpyrrole > 1-methylpyrazole ~ 1-methylimidazole > pyrrole > pyrazole ~ imidazole. This differs markedly from the observed BDE order (see Table 3) and suggests that the influence of the polarizability of the ligand is also small. As discussed above, methyl substitution leads to an increase in the polarizability and in the observed binding affinity, but no simple correlation across this family of azoles with polarizability is found. This also suggests that the influence of the polarizability on the binding to these systems is small. Overall, the observed trends in the binding of alkali metal ions to these azole ligands are therefore dominated by the size of the metal ion, and secondarily by the nature of the metal$-$ligand interaction (π vs σ binding) and the dipole moment of the ligand. The quadrupole moment and polarizability of the ligand appear to influence the binding in these systems to only a minor extent.

Correlation of Alkali Metal Ion Binding Affinity with Proton Affinity. Correlation of the alkali metal ion binding energies of the azoles to their proton affinity is also informative. Figure 9 shows that the correlation between the alkali metal ion binding energies and their proton affinities is very good for all six azoles examined here. This linear correlation suggests that the binding is very similar in the protonated and alkali metalated complexes for these systems. This is not surprising for the pyrazole, 1-methylpyrazole, imidazole, and 1-methylimidazole systems as the H^+ and M^+ binding interactions are very similar in nature. In contrast, the binding interactions of H^+ and M^+ with pyrrole and 1-methylpyrrole are quite different, and therefore it is somewhat surprising that a linear correlation is found across all of the azole systems.

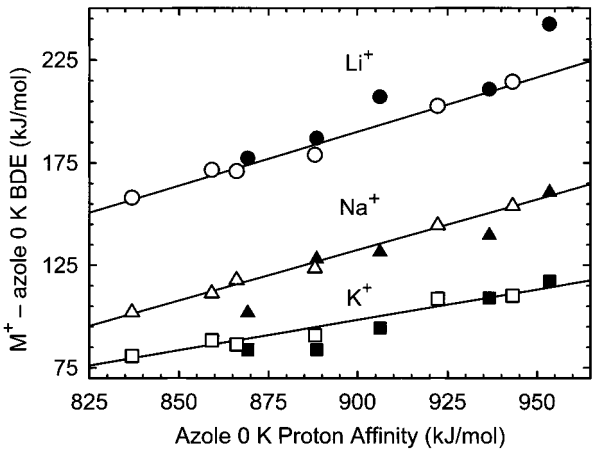

Figure 9. Bond dissociation energies of M^+(azole) (in kJ/mol) versus proton affinity of the neutral azole (in kJ/mol) at 0 K, where M^+ = Li^+ (●, ○), Na^+ (▲, △), and K^+ (■, □), and azole = pyrrole, 1-methylpyrrole, pyrazole, 1-methylpyrazole, imidazole, and 1-methylimidazole. Linear regression analyses of the theoretical values are indicated with solid lines. Proton affinities are taken from the NIST webbook.[33]

Conclusions

The kinetic energy dependences of the collision-induced dissociation of M^+(azole), where $M^+ = Li^+$, Na^+, and K^+ and azole = pyrrole, 1-methylpyrrole, pyrazole, 1-methylpyrazole, and 1-methylimidazole, with Xe are examined in a guided ion beam mass spectrometer. The dominant dissociation process in all cases is loss of the intact azole ligand. Thresholds for these processes are determined after consideration of the effects of reactant internal energy, multiple collisions with Xe, and lifetime effects (by methodology described in detail elsewhere).[4] Insight into the structures and BDEs of the M^+(azole) complexes is provided by ab initio calculations of these complexes performed at the MP2(full)/6-311+G(2d,2p)//MP2(full)/6-31G* level of theory. Excellent agreement between the experimentally determined and theoretically calculated BDEs for the Na^+ and K^+ systems is obtained. The agreement between theory and experiment for the Li^+ systems is not as good. The values measured here are greater than those calculated, and the MADs between these values lie outside of the experimental error estimated for these systems. Several plausible explanations are provided for this discrepancy. Previous literature values for the Li^+ complexes to pyrrole and 1-methylpyrrole are in much better agreement with theory, but literature values for imidazole and 1-methylimidazole appear to be systematically low.[31,32] The high fidelity of our experimental and theoretical results for the Na^+ and K^+ systems suggest that these ligands can act as reliable anchors for the alkali metal cation affinity scales. Thus these systems broaden the range of ligands available as absolute thermochemical anchors. Further, the combined theoretical and experimental results suggest that the size of the metal ion, the nature of the metal$-$ligand interaction (π vs σ binding), and the dipole moment of the ligand are the dominant factors that determine the strength of these noncovalent interactions. The quadrupole moment and polarizability of the ligand obviously influence the binding as well, but to a lesser extent. The present results suggest that pyrrole and 1-methylpyrrole are truly π-excessive N-heterocycles. In contrast, the binding behavior of pyrazole, 1-methylpyrazole, imidazole, and 1-methylimidazole suggest that these ligands are π-deficient N-heterocycles.

Acknowledgment. This work was supported in part by an ASMS Research Award from Micromass.

Supporting Information Available: Tables of vibrational frequencies, average vibrational energies, rotational constants, and MP2(full)/6-31G* geometry optimized structures for neutral, protonated, and alkali metalated azoles and figures showing cross sections for the collision-induced dissociation of M^+(azole) complexes with Xe as well as empirical fits to the M^+ product channels (PDF). This material is available free of charge via the Internet at http://pubs/acs/org.

References and Notes

(1) Rodgers, M. T. *J. Phys. Chem. A* **2001**, *105*, 2374.
(2) Rodgers, M. T.; Armentrout, P. B. *J. Phys. Chem. A* **1997**, *101*, 1238.
(3) Rodgers, M. T.; Armentrout, P. B. *J. Phys. Chem. A* **1997**, *101*, 2614.
(4) Rodgers, M. T.; Ervin, K. M.; Armentrout, P. B. *J. Chem. Phys.* **1997**, *106*, 4499.
(5) Rodgers, M. T.; Armentrout, P. B. *J. Chem. Phys.* **1998**, *109*, 1787.
(6) Rodgers, M. T.; Armentrout, P. B. *Int. J. Mass Spectrom.* **1999**, *185*/*186*/*187*, 359.
(7) Rodgers, M. T.; Armentrout, P. B. *J. Phys. Chem. A* **1999**, *103*, 4955.
(8) Armentrout, P. B.; Rodgers, M. T. *J. Phys. Chem. A* **2000**, *104*, 2238.
(9) Amunugama, R.; Rodgers, M. T. *Int. J. Mass Spectrom.* **2000**, *195*/*196*, 439.
(10) Rodgers, M. T.; Armentrout, P. B. *J. Am. Chem. Soc.* **2002**, *124*, 2678.
(11) Rodgers, M. T.; Stanley, J. R.; Amunugama, R. *J. Am. Chem. Soc.* **2000**, *122*, 10969.
(12) Amunugama, R.; Rodgers, M. T. *J. Phys. Chem. A* **2001**, *105*, 9883.
(13) Rodgers, M. T. *J. Phys. Chem. A* **2001**, *105*, 8145.
(14) Valina, A. B.; Amunugama, R.; Huang, H.; Rodgers, M. T. *J. Phys. Chem. A* **2001**, *105*, 11057.
(15) Vitale, G.; Valina, A. B.; Huang, H.; Amunugama, R.; Rodgers, M. T. *J. Phys. Chem. A* **2001**, *105*, 11351.
(16) Newkome, G. R.; Paudler, W. W. *Contemporary Heterocyclic Chemistry: Syntheses, Reactions, and Applications*; Wiley: New York, 1982.
(17) Pederson, C. J. *J. Am. Chem. Soc.* **1967**, *89*, 7017.
(18) Izatt, R. M.; Nelson, D. P.; Ryting, J. H.; Haymore, B. L.; Christensen, J. J. *J. Am. Chem. Soc.* **1971**, *93*, 1619.
(19) Cartledge, J. D.; Midgley, J.; Petrout, M.; Shanson, D.; Gazzard, B. G. *J. Antimicrob. Chemother.* **1997**, *40*, 517.
(20) Hopewell, P. C. *Semin. Resp. Crit. Care Med.* **1997**, *18*, 471.
(21) Nelson, M. R.; Fisher, M.; Cartledge, J.; Rodgers, T.; Gazzard, B. G. *AIDS* **1994**, *8*, 651.
(22) Cartledge, J. D.; Denning, P. W.; Dupont, B.; Clumeck, N.; Dewit, S.; Midgley, J.; Hawkins, D. A.; Gazzard, B. G. *AIDS* **1998**, *12*, 411.
(23) Lamb, D. C.; Cannieux, M.; Warrilow, A. G. S.; Bak, S.; Kahn, R. A.; Manning, N. J.; Kelly, D. E.; Kelly, S. L.; *Biochem. Biophys. Res. Commun.* **2001**, *284*, 845.
(24) Botcher, T. R.; Beardall, D. J.; Wight, C. A.; Fan, L.; Burkey, T. J. *J. Phys. Chem.* **1996**, *100*, 8802.
(25) Meredith, C.; Russell, T. P.; Mowrey, R. C.; McDonald, J. R. *J. Phys. Chem.* **1998**, *102*, 471.
(26) Guzel, I. A.; Baboul, A. G.; Yap, G. P. A.; Rheingold, A. L.; Schlegel, H. B.; Winter, C. H.; *J. Am. Chem. Soc.* **1997**, *119*, 3387.
(27) Reck, C. E.; Winter, C. H. *Organometallics* **1997**, *16*, 4493.
(28) Guzei, I. A.; Yap, G. P. A.; Winter, C. H. *Inorg. Chem.* **1997**, *36*, 1738.
(29) Yelamos, C.; Heeg, M. J.; Winter, C. H. *Inorg. Chem.* **1998**, *37*, 3892.
(30) Miller, K. J. *J. Am. Chem. Soc.* **1990**, *112*, 8533.
(31) Taft, R. W.; Anvia, F.; Gal, J.-F.; Walsh, S.; Capon, M.; Holmes, M. C.; Hosn, K.; Oloumi, G.; Vasanwala, R.; Yazdani, S. *Pure Appl. Chem.* **1990**, *62*, 17.
(32) Burk, P.; Koppel, I. A.; Koppel, I.; Kurg, R.; Gal, J.-F.; Maria, P.-C.; Herreros, M.; Notario, R.; Abboud, J.-L. M.; Anvia, F.; Taft, R. W. *J. Phys. Chem. A* **2000**, *104*, 2824.
(33) Hunter, E. P.; Lias, S. G. Proton Affinity Evaluation. In *NIST Chemistry WebBook*; NIST Standard Reference Database No. 69; Mallard, W. G., Lindstrom, P. J., Eds.; National Institute of Standards and Technology: Gaithersburg, MD, November 1998; p 20899 (http://webbook.nist.gov).
(34) Gapeev, A.; Yang, C.; Klippenstein, S. J.; Dunbar, R. C. *J. Phys. Chem. A* **2000**, *104*, 3246.
(35) Hoyau, S.; Norrman, K.; McMahon, T. B.; Ohanessian, G. *J. Am. Chem. Soc.* **1999**, *121*, 8864.
(36) McMahon, T. B.; Ohanessian, G. *Chem. Eur. J.* **2000**, *6*, 2931.
(37) Amicangelo, J. C.; Armentrout, P. B. *J. Phys. Chem. A* **2000**, *104*, 11420.
(38) Amunugama, R.; Rodgers, M. T. *J. Phys. Chem. A* (accepted for publication).
(39) (a) Teloy, E.; Gerlich, D. *Chem. Phys.* **1974**, *4*, 417. (b) Gerlich, D. Diplomarbeit, University of Freiburg, Federal Republic of Germany, 1971. (c) Gerlich, D. In State-Selected and State-to State Ion−Molecule Reaction Dynamics, Part I, Experiment; Ng, C.-Y., Baer, M., Eds.; *Adv. Chem. Phys.* **1992**, *82*, 1.
(40) Dalleska, N. F.; Honma, K.; Armentrout, P. B. *J. Am. Chem. Soc.* **1993**, *115*, 12125.
(41) Aristov, N.; Armentrout, P. B. *J. Phys. Chem.* **1986**, *90*, 5135.
(42) Hales, D. A.; Armentrout, P. B. *J. Cluster Sci.* **1990**, *1*, 127.
(43) Ervin, K. M.; Armentrout, P. B. *J. Chem. Phys.* **1985**, *83*, 166.
(44) Dalleska, N. F.; Honma, K.; Sunderlin, L. S.; Armentrout, P. B. *J. Am. Chem. Soc.* **1994**, *116*, 3519.
(45) Schultz, R. H.; Armentrout, P. B. *J. Chem. Phys.* **1992**, *96*, 1046.
(46) Schultz, R. H.; Crellin, K. C.; Armentrout, P. B. *J. Am. Chem. Soc.* **1992**, *113*, 8590.
(47) Khan, F. A.; Clemmer, D. C.; Schultz, R. H.; Armentrout, P. B. *J. Phys. Chem.* **1993**, *97*, 7978.
(48) Fisher, E. R.; Kickel, B. L.; Armentrout, P. B. *J. Phys. Chem.* **1993**, *97*, 10204.
(49) (a) Beyer, T. S.; Swinehart, D. F. *Comm. Assoc. Comput. Machines* **1973**, *16*, 379. (b) Stein, S. E.; Rabinovitch, B. S. *J. Chem. Phys.* **1973**, *58*, 2438; *Chem. Phys. Lett.* **1977**, *49*, 1883.
(50) (a) Pople, J. A.; Schlegel, H. B.; Raghavachari, K.; DeFrees, D. J.; Binkley, J. F.; Frisch, M. J.; Whitesides, R. F.; Hout, R. F.; Hehre, W. J. *Int. J. Quantum Chem. Symp.* **1981**, *15*, 269. (b) DeFrees, D. J.; Mclean, A. D. *J. Chem. Phys.* **1985**, *82*, 333.
(51) Waage, E. V.; Rabinovitch, B. S. *Chem. Rev.* **1970**, *70*, 377.
(52) Chesnavich, W. J.; Bowers, M. T. *J. Phys. Chem.* **1979**, *83*, 900.
(53) Armentrout, P. B.; In *Advances in Gas-Phase Ion Chemistry*; Adams, N. G., Babcock, L. M., Eds.; JAI; Greenwich, CT, 1992; Vol. 1, pp 83−119.
(54) See, for example, Sunderlin, L. S.; Armentrout, P. B. *Int. J. Mass Spectrom. Ion Processes* **1989**, *94*, 149.
(55) More, M. B.; Glendening, E. D.; Ray, D.; Feller, D.; Armentrout, P. B. *J. Phys. Chem.* **1996**, *100*, 1605.
(56) Ray, D.; Feller, D.; More, M. B.; Glendening, E. D.; Armentrout, P. B. *J. Phys. Chem.* **1996**, *100*, 16116.
(57) Meyer, F.; Khan, F. A.; Armentrout, P. B. *J. Am. Chem. Soc.* **1995**, *117*, 9740.
(58) See, for example: Figure 1 in Dalleska et al.[40]
(59) Armentrout, P. B.; Simons, J. *J. Am. Chem. Soc.* **1992**, *114*, 8627.
(60) Frisch, M. J.; Trucks, G. W.; Schlegel, H. B.; Scuseria, G. E.; Robb, M. A.; Cheeseman, J. R.; Zakrzewski, V. G.; Montgomery, J. A., Jr.; Stratmann, R. E.; Burant, J. C.; Dapprich, S.; Millam, J. M.; Daniels, A. D.; Kudin, K. N.; Strain, M. C.; Farkas, O.; Tomasi, J.; Barone, V.; Cossi, M.; Cammi, R.; Mennucci, B.; Pomelli, C.; Adamo, C.; Clifford, S.; Ochterski, J.; Petersson, G. A.; Ayala, P. Y.; Cui, Q.; Morokuma, K.; Malick, D. K.; Rabuck, A. D.; Raghavachari, K.; Foresman, J. B.; Cioslowski, J.; Ortiz, J. V.; Stefanov, B. B.; Liu, G.; Liashenko, A.; Piskorz, P.; Komaromi, I.; Gomperts, R.; Martin, R. L.; Fox, D. J.; Keith, T.; Al-Laham, M. A.; Peng, C. Y.; Nanayakkara, A.; Gonzalez, C.; Challacombe, M.; Gill, P. M. W.; Johnson, B.; Chen, W.; Wong, M. W.; Andres, J. L. Gonzalez, C.; Head-Gordon, M.; Replogle, E. S.; Pople, J. A. *Gaussian 98*, revision A.9; Gaussian, Inc.: Pittsburgh, PA, 1998.
(61) Møller, C.; Plesset, M. S. *Phys. Rev.* **1934**, *46*, 618.
(62) Foresman, J. B.; Frisch, Æ. *Exploring Chemistry with Electronic Structure Methods*, 2nd ed.; Gaussian: Pittsburgh, PA, 1996.
(63) Boys, S. F.; Bernardi, R. *Mol. Phys.* **1979**, *19*, 553.
(64) Van Duijneveldt, F. B.; van Duijneveldt-van de Rijdt, J. G. C. M.; van Lenthe, J. H. *Chem. Rev.* **1994**, *94*, 1873.
(65) Lifshitz, C. *Adv. Mass Spectrom.* **1989**, *11*, 113.
(66) Figures were generated using the output of Gaussian 98 geometry optimizations in Hyperchem Computational Chemistry Software Package, Version 5.0, Hypercube Inc., 1997.
(67) Bartlett, R. J. *Annu. Rev. Phys. Chem.* **1981**, *32*, 359.
(68) Hehre, W. J.; Radom, L.; Schleyer, P. v. R.; Pople, J. A. *Ab Initio Molecular Orbital Theory*; Wiley: New York, 1986.
(69) Mullikan populations, calculated at the MP2/6-311+G(2d,2p) level of theory.